Advanced Studies in Theoretical Physics
Vol. 15, 2021, no. 4, 187 - 199
HIKARI Ltd, www.m-hikari.com
https://doi.org/10.12988/astp.2021.91546

Variation of Potential Surface Inclination and Bound State Creation Induced by Laser Phase Along the Reaction Path in Ion-Molecule Reactions: Application to $Na^+ + CH_4$

Hassan Talaat

Physics Dept., Faculty of Science
Ain Shams University, Cairo, Egypt

El-Wallid S. Sedik* and M. Tag El-Din Kamal

Theoretical Physics Dept.
National Research Center, Dokki, Giza, Egypt
* Corresponding author

Abstract

Laser ion-molecule reaction interaction through both polarizability and dipole moment contribution leads to intersection in potential energy surface along the reaction path, polarizability is maximum at (s=4.5 a.u.) and dipole changes at (s=1 a.u.) defining a virtual transition state. We will show here by using gauge representation for wave length λ=20.6μm, Intensity $I=5\times10^{11}$ W/cm^2 till $I=5\times10^{13}$ W/cm^2, that the laser induced potential energy surface can decrease in height along the reaction path with possibility of creating bound states in the virtual transition state. We illustrate such effects for the Na H + $CH_3^+ \leftrightarrow Na^+ + CH_4$ reaction which takes the form of inverted Morse (without a barrier) using ab-initio methods for calculating the reaction path, electric properties of the ion-molecule reaction.

Keywords: Intense laser fields; dipole moment; polarizability; reaction path; unrestricted second order Møller-Plesset calculations (UMP2); ion-molecule reaction; potential energy surface intersection

1. Introduction

Advances in laser technology opens up a new field of research, the nonlinear, nonperturbative interaction of molecules with intense ultrashort pulses.[1] Manipulation of the amplitude and the relative phase of the laser pulses leads to coherent control of molecular radiative processes.[2] Recently, ultrashort pulses have been created with phase stabilized carrier-envelopes[3,4] thus allowing for the study of absolute phase pulse effects such as asymmetric ionization leading to measurement of the absolute phase itself.[5] A quantum mechanical approach was used to show that barrier suppression [6,7,8,9] and modification of non adiabatic effects [10] is a general phenomenon in the presence of intense IR laser fields.
Potential energy surface intersection induced by laser[11] is important in ion-molecule reactions as well as in charge transfer processes. In the present work we focus on the $Na^+ + CH_4$ ion molecule reaction with the goal of studying the effect of an intense laser field on the permanent dipole moment of this and other similar systems.[12] Using ab-initio methods, we calculate the energy of the reaction path, and the permanent dipole moment, polarizability along the reaction path. We find that the permanent dipole moment is linear with the reaction path and this moment can vanish at critical distances and the polarizability is maximum in the transition state. This result implies maximum electron delocalization at this point along the reaction path. We restrict ourselves to a 1-D model using the electric field gauge to show the influence of the laser field on the potential surfaces of ion-molecule systems which leads to potential surface intersection as shown in Figs.(2-5). This allows to incorporate the laser interaction directly into the potential surface, thus leading to an analytical formula to describe the laser-reaction path interactions. Section 2 explains the theory that leads to potential surface intersection. Section 3 explains the computational method. Section 4 demonstrates the results and discussion. Section 5 is the conclusion.

2. Laser Ion-Molecule Interaction

The standard description of laser-particle interaction starts from the classical electric-field particle interaction which by successive unitary transformations on the molecular time-dependent Schrödinger equation, TDSE, leads to various representations (gauges), where particle -radiative couplings have different frequency dependencies.[13] Since we shall consider 1-D reaction paths with coordinates $-\infty \leq s \leq \infty$, the corresponding TDSE with linear dipole moment $\mu(s)= \mu_o s$ and polarizability $\alpha_{zz}(s)$ can be written as:

$$i\frac{\partial\psi(s,t)}{\partial t}=\hat{H}\psi(s,t)=\left[\frac{p_s^2}{2m_s}+V(s)+\mu_o(s)\mathcal{E}(t)+\frac{\alpha_{zz}(s)}{2}\mathcal{E}^2(t)\right]\psi(s,t), \quad (1)$$

$\psi(s,t)$ is the wavefunction for propagation of the relative motion of a nuclear wavepacket as a function of time along the reaction coordinate s which defines a potential V(s) to be calculated by ab-initio methods.

The system under investigation will be the ion-molecule reaction [14] and / or the reverse,

$$Na\ H + CH_3^+ \leftrightarrow Na^+ + CH_4 \quad (2)$$

Thus in the center of mass system the reduced mass M_s will be nearly constant due to the much smaller mass of the transferred proton. The ab-initio calculations below will show that the dipole moment of reaction (2) is indeed linear with s so that Eq. (1) with M_s constant will be an excellent approximation to represent the motion along the reaction path s in the presence of a laser field $\mathcal{E}(t)=E_o\cos\omega t$, with amplitude E_o and frequency ω. The laser-particle interaction in (1) is written in the dipole approximation ($s/\lambda << 1$), i.e., the long wavelength approximation. As an example current intense near IR lasers operate at 800nm whereas our simulations will be in the range $|s| \leq 1$ nm.

We shall be studying detailed variations of the potential surface $V(s)$, dipole moment $\mu(s)$, and polarizability $\alpha(s)$, along the reaction path s for $Li^+ + CH_4$. In the presence of strong fields of amplitude $\mathcal{E}(t) = \mathcal{E}_o \cos(\omega t + \phi)$, where $\mathcal{E}_o$ is the maximum amplitude, ω the frequency, and ϕ the phase, high order radiative interactions will distort the surfaces. Nevertheless, an upper limit to the strength of the field is necessary in order to avoid ionization. In IR long wavelength fields, electronic ionization can be treated as a tunneling model.[15] Thus, using direct current (DC) tunneling theory,[16] one can estimate the tunneling ionization rate $w(t)$ for a static electric field amplitude $\mathcal{E}$[17],

$$w(t)=4\omega_o\left[\frac{E_i}{E_h}\right]^{5/2}\frac{E_a}{E(t)}\exp\left[-\frac{2}{3}\left[\frac{E_i}{E_h}\right]^{3/2}\frac{E_a}{E(t)}\right] \quad (3)$$

where ω_o is the atomic frequency unit ($\omega_o = 4\times10^{16}\ s^{-1}$), E_h and E_i are the ionization potentials of hydrogen and the atom in question and E_a is the atomic unit of the electric field.

Below this threshold, non-linear interactions with the electric field will occur, leading to a general dipole moment expression:[18]

$$\mu = \mu_o + \frac{1}{2}\alpha\mathcal{E} + \frac{1}{6}\beta\mathcal{E}^2 + \frac{1}{24}\gamma\mathcal{E}^3 + ... \quad (4)$$

where μ_o is the permanent dipole moment, α the polarizability tensor, and β and γ are the first and second hyperpolarizability tensors. The essential parameters for the theoretical description of the alignment of molecules in the non resonant case are μ_o and α [19] for intensities not exceeding $I=3\times10^{13}$ W cm^{-2}. Beyond this intensity, the hyperpolarizability expansion fails already for the hydrogen atom whereas below this intensity, contributions from β and γ are negligible.[20]. We conclude from this that at intensities below 3×10^{13} W cm^{-2} in the IR region, ionization is negligible and the field-perturbative expansion Eq.(4) for the total dipole moment is adequate up to the second term $\frac{1}{2}\alpha\mathcal{E}$, i.e. including only polarizability.

Having established the limits of applicability of perturbative approaches to laser- molecule interaction, we describe the laser-molecule Hamiltonian by retaining only the dipole μ (s)) and the polarizability α (s) along the reaction path s, following,[18]

$$\hat{H}_L = -\mu(s)\mathcal{E}(t)\cos\theta - \frac{\mathcal{E}^2(t)}{2}\left[\alpha_{\parallel}(s)\cos^2\theta + \alpha_{\perp}(s)\sin^2\theta\right] \quad (5)$$

where $\alpha_{\parallel} = \alpha_{zz}$ and $\alpha_{\perp} = \alpha_{xx}$. Assuming $\mathcal{E}(t) = \mathcal{E}_o\cos(\omega t + \phi)$ and retaining the polarizability component, $\alpha_{zz}(s)$, parallel to the reaction path s, (as shown later both μ (s) and the parallel component $\alpha_{zz}(s)$ will dominate at the transition state s = 0), we can re-write Eq.(5) as:

$$\hat{H}_L = -\frac{1}{4}\alpha_{zz}(s)\mathcal{E}_o^2 - \mu(s)\mathcal{E}_o\cos(\omega t + \phi) - \frac{1}{4}\alpha_{zz}(s)\mathcal{E}_o^2\cos(2\omega t + 2\phi)\,. \quad (6)$$

Thus, the parameters $\mu(s)\mathcal{E}_\circ$ and $\frac{1}{4}\alpha_{zz}(s)\mathcal{E}_o^2$ determine the relative amplitude in the present case and ϕ remains the relative phase in Eq.(5). This creates *periodic* but *non-symmetric* electric fields which induce asymmetric concomitant dissociation and ionization. In the present work we will examine the effect of the effective two-colour fields on the reaction path based on Eq.(5) which will be dominant in the transition state region. It is to be noted immediately that for negative dipoles μ, destructive interferences will occur at some phase ϕ.

At high frequencies, the Hamiltonian in Eq.(5) reduces to a frequency-independent Stark shift $-\frac{1}{4}\alpha_{zz}(s)\mathcal{E}_o^2$. We will examine rather the quasi-static low frequency limit and choose the instantaneous period ωt = 0, so that the effective potential along the reaction path is defined as:

$$V = V(s) - \mu(s)\,\mathcal{E}_o \cos(\phi) - \frac{1}{2}\alpha_{zz}(s)\mathcal{E}_o^2 \cos^2(\phi)\,. \tag{7}$$

The parameters $\mu(s)$ and $\alpha(s)$ are next calculated by ab-initio methods in order to illustrate the laser-molecule interaction along the reaction path, based on (Eq. 7) and this will be shown to be the dominant interaction in the transition state region.
This is to be compared to the two colour coherent superposition of laser pulses used to study in detail laser control of dissociative ionization,[21,22]

$$\mathcal{E}(t) = \mathcal{E}_o(t)\left[\cos(\omega t) + f\,\cos(2\omega t + \phi)\right], \tag{8}$$

for a given frequency ω, relative phase ϕ and relative amplitude f.

3. Computational Methods

All calculations were carried out using the unrestricted second-order Møller-Plesset perturbation theory[23] including excitations from inner shell electrons and using a large polarized basis set supplemented with diffuse functions on all atoms [UMP2(full)/6-311++G(2*d*,2*p*)]. The [UMP2(full)/6-311++G(2*d*,2*p*)] appears reasonable as it gives the real geometry at reasonable time, it is not time consuming. Our optimization using the much larger basis set results in a linear C_{3v} transition structure and correct values for the dipole moment and polarizability, although the reaction lacks transition state, we believe that there is a "virtual transition state" where the polarizability is maximum which defines an electron delocalization at s= 4 a.u. in which the dipole moment changes sign. In other words polarizability defines a transition state.

All geometry optimizations, potential energy scans, and reaction path tracings, were also carried out at the same computational level. Geometry optimizations carried out in this work are full unconstrained energy minimizations with respect to all geometric parameters. Electronic structure calculations were performed using the Gaussian 2003 program.[24] Very tight convergence criteria for the (UMP2) calculation as well as for geometry optimizations were set in all calculations. The spin contamination was found to be negligible along the reaction paths. Starting from the respective structure, the reaction path was followed downhill along the intrinsic reaction coordinates (IRC)[25,26] using the algorithm of Gonzalez and Schlegel[27,28] to trace the reaction path.

4. Results and Discussions

An inverted repulsive Morse potential V(s) was obtained by ab-initio quantum chemical calculations using configuration interaction at the level of MP2 which is

described in the previous section. The potential has asymptotic energies of reactants Na H + CH_3^+ at s=0 and products Na^+ + CH_4 at s = 12 a.u. where s is the reaction coordinate. The system lacks transition state reaction (2) along the reaction coordinate s. It is to be noticed that the dipole moment changes at s= 1.5 a.u. The polarizability is maximum at s= 4.5+ au. both the dipole and polarizability defines a virtual transition state for Na H + $CH_3^+ \leftrightarrow Na^+ + CH_4$ reaction.[11,29,30] In the presence of intense IR laser pulses not exceeding intensities $\approx 10^{13}$ W/cm^2, the absolute phase of the electric field determine the dipole mediated field interaction dominates. The energies can increase or decrease or cross as a function of the absolute phase of the laser field.[7,8] Figures 2-7 shows the effect of the laser phase on molecules.[18,19] The dotted curve is the potential energy surface in the absence of the laser field while the solid curve is the potential energy surface in the presence of the laser field. In the intensity of 10^{12} -10^{13} W/cm^2 controlling of the potential energy surface through laser phase was achieved at $\theta = 0,\pi/4,\pi/3, 2\pi/3, \pi$.

Figure 2-4 shows the effect of only the polarizability on the potential surface. In the intensity $1x10^{11}$, $1x10^{12}$ W/cm^2 the potential along the reaction coordinate shows no change at $\theta = 0,\pi/4,\pi/3,2\pi/3,\pi$. By increasing the intensity to $3x10^{12}$,$5x10^{12}$W/cm^2 the potential decreases in height at $\theta = 0, \pi/4, \pi$ until it reaches a minimum value at intensity $1x10^{13}$ $\theta=\pi$. In the range $3x10^{13}$, $5x10^{13}$, $\theta = 0,\pi/4,2\pi/3,\pi$ the dressed potential became curved showing a possibility of bound states in the range s=4.5-6.5 a.u.

For the dipole moment and polarizability contribution as shown in fig.5-7 the intensity $5x10^{11}$ W/cm^2 the potential along the reaction coordinate shows no change. In the intensity $1x10^{12}$, $3x10^{12}$, $5x10^{12}$ W/cm^2 the potential along the reaction coordinate deceases in height and crosses with the original one $\theta = \pi$, the dressed potential became curved and lower to the original potential and interfere at $\theta = \pi$ towards the end of the reaction coordinate.

5. Conclusion

We have studied the change in energetic and electric properties (dipole moment and polariability) along the reaction paths of the Na^++CH_4 reactions. We have added the laser molecule interaction to the field free ab initio potentials using eq. 7 for $\theta = 0, \pi/4,\pi/3,2\pi/3,\pi$, Assuming $\omega t=0$ and with an upper limit not exceeding 10^{13} W/cm^2 to avoid ionization for the reaction. We found that Na^++ CH_4 that surface crossing becomes possible where dipole moment changes sign and polarizability is maximum which suggests control of chemical reactions. These crossings are important in ion-molecule reactions especially charge transfer. The advent of phase stabilized near femtosecond pulses should allow for the observation of dipole and polarizability contribution to the laser molecule interaction as predicted by eq. 7, provided the dura-

tion of the pulse and collisional interaction at the transition state will be of comparable magnitude. One will expect alignment and therefore guiding of the reaction along the linear minimum energy path.

References

[1] A. D. Bandrauk and H. Kono, in: *Advances in Multiphoton Processes and Spectroscopy*, S. H. Lin (ed.), Vol. 15, World Scientific, Singapore (2003), p.150.
[2] M. Shapiro and P. Brumer, *Principles of the Quantum Control of Molecular Processes*, Wiley - Interscience, NY, 2003. https://doi.org/10.1002/9783527639700
[3] G. Paulus et al., *Phys. Rev. Lett*., **91** (2003), 253004.
[4] V. S. Yakovlev et al., *Appl. Phys. B***, 76** (2003), 329.
[5] S. Chelkowski and A. D. Bandrauk, *Phys. Rev. A***, 65** (2002), 061802. https://doi.org/10.1103/physreva.65.023403
[6] A. E. Orel and W. H. Miller, *Chem. Phys. Lett*., **57** (1978), 362; *J. Chem. Phys.*, **73** (1980), 241. https://doi.org/10.1016/0009-2614(78)85526-2 , https://doi.org/10.1063/1.439923
[7] A. E. Orel and W. H. Miller, *J. Chem. Phys*., **70** (1979), 4393. https://doi.org/10.1063/1.438013
[8] T. Brabec, F. Krausz, *Rev. Mod. Phys*., **72** (2000), 545. https://doi.org/10.1103/revmodphys.72.545
[9] A. D. Bandrauk, M.S. Child, *Molec. Phys*., **19** (1970), 95. https://doi.org/10.1080/00268977000101041
[10] D. G. Truhlar and A. D. Isaacson, *J. Chem. Phys*., **77** (1982), 3516. https://doi.org/10.1063/1.444297
[11] M. Tag El-Din Kamal, El-wallid S. Sedik, and Hassan Talaat, *Z. Phys.Chem*., **222** (2008), 1693. https://doi.org/10.1524/zpch.2008.5435
[12] V. Ramatmurthy et al., *Chem. Commun*., (1987), 2003.
[13] S. Chelkowski and A. D. Bandrauk, *Opt. Lett*., **29** (2004), 13. https://doi.org/10.1364/ol.29.001557
[14] M.C. Heaven, in: *Chemical Dynamics in Extreme Environments*, R.A. Dressler (ed.),World Scientific, Singapore (2000).
[15] L. V. Keldysh, *Sov. Phys., J. Exp. Theor. Phys.*, **20** (1965), 1307.
[16] P. B. Corkum, N. H. Burnett, F. Brunel, *Phys. Rev. Lett.*, **62** (1989), 1259. https://doi.org/10.1103/physrevlett.62.1259
[17] L. D. Landau and E. M. Lifshitz, *Quantum Mechanics*, Pergamon Press, NY, 1965, 276p.
[18] C. Dion, A. Keller, O. Atabek, and A. D. Bandrauk, *Phys. Rev. A*, **59** (1999), 1382. https://doi.org/10.1103/physreva.59.1382
[19] H. Stapelfeldt, T. Seideman, *Rev. Mod. Phys*., **75** (2003), 543. https://doi.org/10.1103/revmodphys.75.543

[20] L. Pan, K. T. Taylor, C. W. Clark, *J. Opt. Soc. Am*., **B7** (1990), 509. https://doi.org/10.1364/josab.7.000509
[21] A. D. Bandrauk and S. Chelkowski, *Phys. Rev. Lett*., **84** (2000), 3562. https://doi.org/10.1103/physrevlett.84.3562
[22] J. Levesque, S. Chelkowski, and A. D. Bandrauk, *J. Phys. Chem*., **107** (2003), 3457. https://doi.org/10.1021/jp022044v
[23] C. Moller and M. S. Plesset, *Phys. Rev*., **46** (1934), 618. https://doi.org/10.1103/physrev.46.618
[24] M. J. Frisch et al., *Gaussian2003,* Gaussian Inc., Pittsburgh PA, 2003.
[25] K. Fukui, *J. Phys. Chem*., **74** (1970), 4161. https://doi.org/10.1021/j100717a029
[26] K. Fukui, *Acc. Chem. Res*., **14** (1981), 363. https://doi.org/10.1021/ar00072a001
[27] C. Gonzalez and H. B. Schlegel, *J. Chem. Phys*., **90** (1989), 2154. https://doi.org/10.1063/1.456010
[28] C. Gonzalez and H. B. Schlegel, *J. Phys. Chem*., **94** (1990), 5523. https://doi.org/10.1021/j100377a021
[29] Hassan Talaat, Ali H. Moussa, M. Shalaby, El-wallid S. Sedik, M. Tag El-Din Kamal, *Russ. J.Phys. Chem*., **87** (2013), 454. https://doi.org/10.1134/s0036024413030369
[30] M. Tag El-Din Kamal, El-wallid S. Sedik, Hassan Talaat, *J. Structural Chem*., **59** (2018), 20. https://doi.org/10.1134/s0022476618010043

Figure 1. Plot of the potential energy surface of the Na-H + CH_3^+ → Na^+ + CH_4 reaction: repulsive inverted Morse; b) Dipole moment μ(s) along the reaction path; c) polarizability component α_{zz}(s) along the reaction path.

1a)

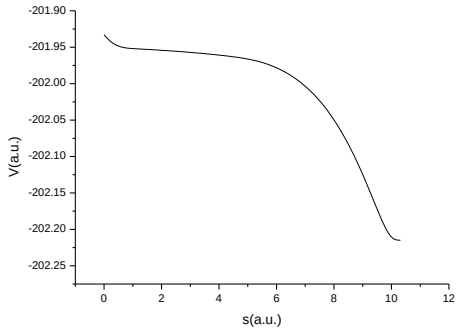

1b)

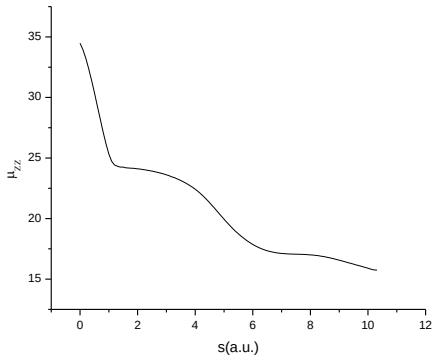

1c)

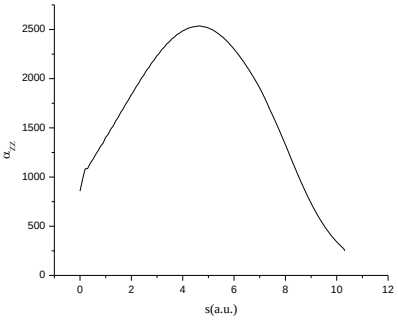

Figure 2. Snapshots of the energy profile along the reaction coordinate plus inclusion of the polarizability for Na H + $CH_3^+ \rightarrow Na^+ + CH_4$. $\lambda = 20.6$ μm.
$I = 1\times 10^{12}$ W/cm^2. a) $\theta = \pi/4$, b) $\theta=\pi$.

2a)

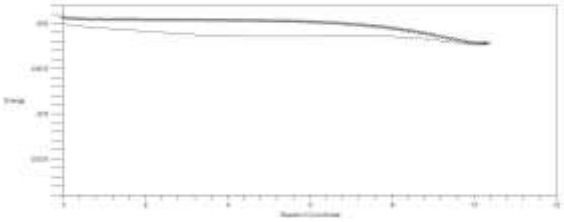

2b)

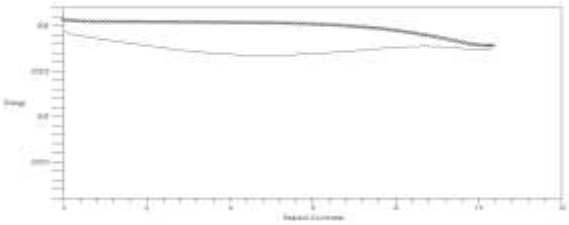

Figure 3. Snapshots of the energy profile along the reaction coordinate plus inclusion of the polarizability for Na H + $CH_3^+ \rightarrow Na^+ + CH_4$. $\lambda = 20.6$ μm.
$I = 3\times 10^{12}$ W/cm^2. a) $\theta = \pi$, b) $\theta = 2\pi/3$.

3a)

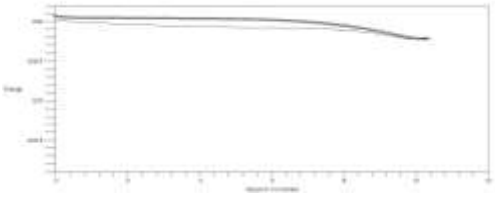

3b)

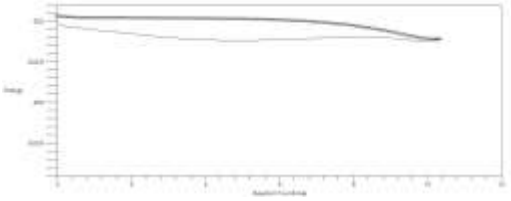

Figure 4. Snapshots of the energy profile along the reaction coordinate plus inclusion of polarizability for Na H + $CH_3^+ \rightarrow Na^+ + CH_4$. $\lambda = 20.6$ μm.
$I = 5\times 10^{12}$ W/cm^2. a) $\theta = \pi$, b) $\theta = \pi/3$.

4a)

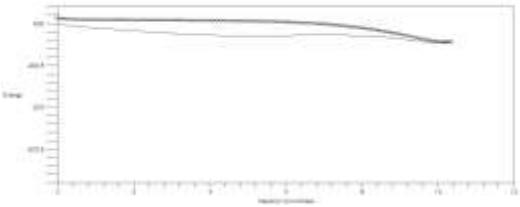

4b)

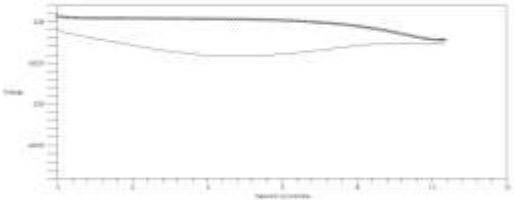

Figure 5. Snapshots of the energy profile along the reaction coordinate plus inclusion of dipole moment and polarizability for Na H + $CH_3^+ \rightarrow Na^+ + CH_4$. $\lambda = 20.6$ μm. $I = 1 \times 10^{13}$ W/cm^2. a) $\theta = 0$, b) $\theta = \pi/4$, c) $\theta = \pi/3$, d) $\theta = \pi$.

5a)

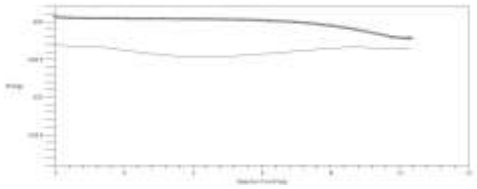

5b)

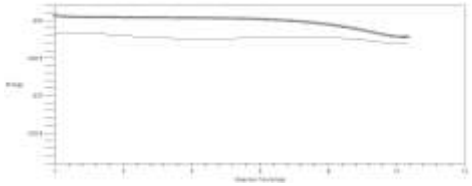

5c)

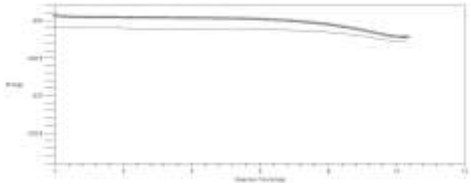

5d)

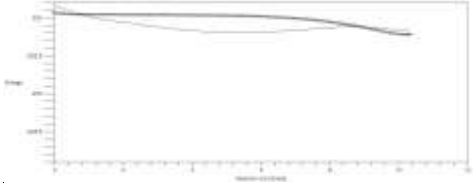

Figure 6. Snapshots of the energy profile along the reaction coordinate plus inclusion of dipole moment and polarizability for Na H + $CH_3^+ \rightarrow Na^+ + CH_4$. $\lambda = 20.6$ μm. $I = 3\times 10^{13}$ W/cm^2. a) $\theta = 0$, b) $\theta = \pi/4$, c) $\theta = \pi/3$, d) $\theta = 2\pi/3$,e) $\theta = \pi$.

6a)

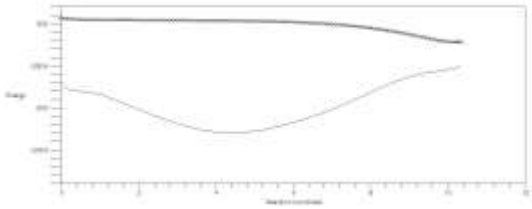

6b)

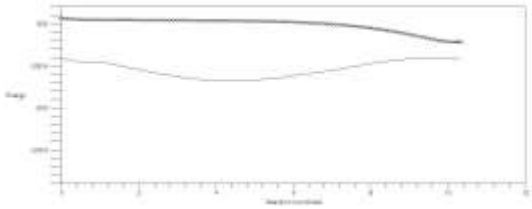

6c)

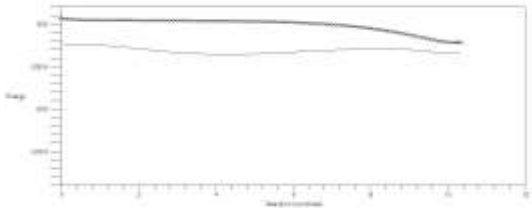

6d)

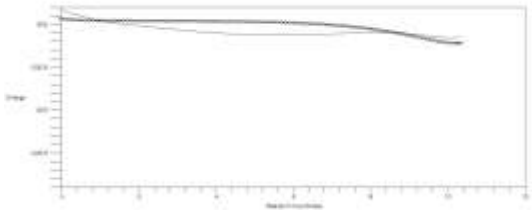

6e)

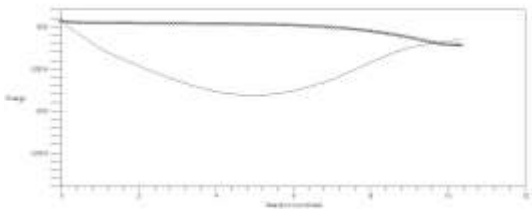

Figure 7. Snapshots of the energy profile along the reaction coordinate plus inclusion of dipole moment and polarizability for Na H + $CH_3^+ \rightarrow Na^+ + CH_4$. $\lambda = 20.6$ μm. $I = 5\times 10^{13}$ W/cm^2. a) $\theta = 0$, b) $\theta = \pi/4$, c) $\theta = \pi/3$, d) $\theta = 2\pi/3$,e) $\theta = \pi$.

7a)

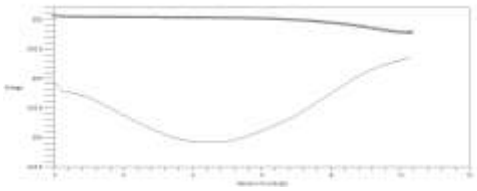

7b)

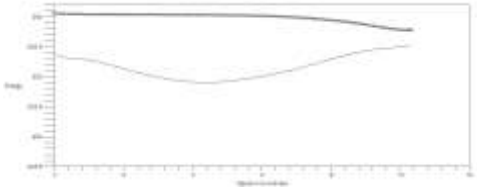

7c)

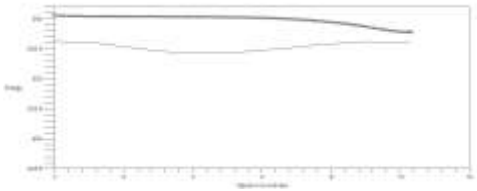

7d)

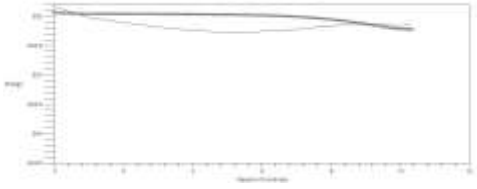

7e)

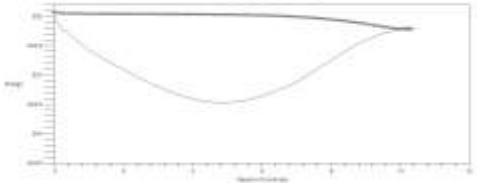

Received: April 5, 2021; Published: May 8, 2021